Published in final edited form as:
Stem Cells. 2011 May ; 29(5): 777–790. doi:10.1002/stem.625.

Assessment of the Myogenic Stem Cell Compartment Following Transplantation of Pax3/Pax7-Induced Embryonic Stem Cell-Derived Progenitors

Radbod Darabi[1], **Filipe N. C. Santos**[2], **Antonio Filareto**[1], **Weihong Pan**[1], **Ryan Koene**[1], **Michael A. Rudnicki**[3], **Michael Kyba**[1], and **Rita C. R. Perlingeiro**[1,*]

[1]Lillehei Heart Institute, Department of Medicine, University of Minnesota, Minneapolis, MN, USA

[2]Department of Anesthesiology, State University of Campinas, Campinas, SP, Brazil

[3]Department of Medicine, Ottawa Health Research Institute, University of Ottawa, Ottawa, ON, Canada

Abstract

An effective long-term cell therapy for skeletal muscle regeneration requires donor contribution to both muscle fibers and the muscle stem cell pool. Although satellite cells have these abilities, their therapeutic potential so far has been limited due to their scarcity in adult muscle. Myogenic progenitors obtained from Pax3-engineered mouse embryonic stem (ES) cells have the ability to generate myofibers and to improve the contractility of transplanted muscles *in vivo*, however whether these cells contribute to the muscle stem cell pool and are able to self-renew *in vivo* is still unknown. Here we addressed this question by investigating the ability of Pax3, which plays a critical role in embryonic muscle formation, and Pax7, which is important for maintenance of the muscle satellite cell pool, to promote the derivation of self-renewing functional myogenic progenitors from ES cells. We show that Pax7, like Pax3, can drive the expansion of an ES-derived myogenic progenitor with significant muscle regenerative potential. We further demonstrate that a fraction of transplanted cells remains mononuclear, and displays key features of skeletal muscle stem cells, including satellite cell localization, response to re-injury and contribution to muscle regeneration in secondary transplantation assays. The ability to engraft, self-renew, and respond to injury provide foundation for the future therapeutic application of ES-derived myogenic progenitors in muscle disorders.

Keywords

ES cells; *Pax7/Pax3*; *satellite cells*; *self-renewal*; *skeletal muscle progenitors*

[*]Correspondence should be addressed to *Rita C. R. Perlingeiro*. Mailing address: Lillehei Heart Institute and Department of Medicine, University of Minnesota, 312 Church St. SE, Minneapolis, MN 55455, USA Phone: 612.625.4984; Fax: 612.624.8118 perli032@umn.edu.

Author Contributions: R.D.: Conception and design, performed experiments, collection of data, data analysis and interpretation, manuscript writing; F.N.C.S.: Conception and design, performed experiments, collection of data; A.F.: Conception and design, performed experiments, collection of data; W.P.: performed experiments, collection of data; R.K.: performed experiments; M. R.: Provision of study material; M.K.: Provision of study material, data analysis and interpretation; R.C.R.P.: Conception and design, financial support, data analysis and interpretation, manuscript writing, final approval of manuscript.

DISCLOSURE OF POTENTIAL CONFLICTS OF INTEREST The authors indicate no potential conflicts of interest.

INTRODUCTION

Skeletal muscle is well recognized for its exceptional regenerative capacity. This tissue is comprised of terminally differentiated specialized postmitotic contractile myofibers, myogenic precursors or myoblasts, and a pool of muscle stem cells, known as satellite cells, located beneath the basal lamina of each myofiber[1] that are particularly responsible for postnatal muscle growth. In mature skeletal muscle, these cells are normally in a quiescent state, being activated in response to muscle damage or disease. Activated satellite cells give rise to proliferating myoblasts, which then fuse to existing necrotic muscle fibers or together to form new myofibers with central nuclei[2–4]. Satellite cells can be defined by their position and phenotypically, by the expression of specific surface markers including M-cadherin[5], c-Met[5], CD34[6, 7], syndecan-4[8], and more importantly, Pax7, a paired box homeodomain-containing transcription factor[9, 10]. It has been demonstrated that following the activation and proliferation of satellite cells, a small subset of cells do not undergo the terminal differentiation pathway, but retain the ability to go back to a quiescent state and thus preserve the satellite cell pool[11–13].

This well orchestrated system of maintaining muscle function throughout life can be disturbed by pathological conditions, in particular muscular dystrophies. In the case of Duchenne Muscular Dystrophy (DMD), in which myofibers are dysfunctional due to the lack of Dystrophin, repetitive cycles of regeneration/degeneration culminate in exhaustion of the satellite cell pool and loss of functional myofibers, which over time are replaced by fibrotic and adipose tissue[14–18]. Although no effective treatment is available at present, one attractive therapeutic approach is to use cell based therapies to promote muscle regeneration. Although satellite cells represent the ideal cell population to be utilized since transplantation of these cells results not only in efficient muscle regeneration but also in engraftment of the satellite cell pool[19–23], a number of caveats limit their therapeutic application. The major challenge in applying these cells for clinical purposes is to obtain enough cells for transplantation since activation and *in vitro* expansion diminishes their engraftment ability[20]. A similar problem has been observed for murine and human hematopoietic stem cells[24–26].

Because ES cells are pluripotent and can be extensively expanded in culture while maintaining their self-renewal and multi-lineage differentiation potential, an ES cell-based therapy has unique advantages. A hurdle is that upon *in vitro* differentiation of ES cells into embryoid bodies (EBs), skeletal myogenic progenitors are generated very inefficiently with only a minority of cells expressing myogenic markers. This is probably due to the scarcity of paraxial mesoderm and lack of appropriate inductive signals within EBs. Regulated expression of Pax3, a key regulator of embryonic myogenesis, can bypass this deficiency and generate a significant number of early myogenic progenitors, which are endowed with substantial regenerative capacity and the ability to restore muscle function following their engraftment in dystrophic mice[27]. The extensive *in vitro* self-renewal capacity of Pax3/ES-derived cells as well as the persistence of their engraftment after systemic delivery points to the possibility of self-renewal of these cells in the recipient.

In this study, we sought to determine whether ES-derived myogenic progenitors, in addition to their efficient capacity to generate functional myofibers, also have the ability to seed the muscle stem cell pool. Because of the unique role of Pax7 in postnatal satellite cell maintenance, we directly compare muscle progenitors derived by Pax3 induction with those derived by Pax7 induction. By assessing *in situ* localization, the ability to respond to re-injury after primary engraftment, and the ability to engraft secondary recipients, we find that both Pax3 and Pax7 promote the derivation of a progenitor population with the ability to seed the muscle stem cell compartment.

MATERIAL and METHODS

Generation of an inducible Pax7 ES cell line

Pax7-expressing vector was provided by Michael Rudnicki[28]. Pax7 fragment (1599 bp) was cut from its carrying vector (pBRIT) using EcoRI and XbaI, and then subcloned into the P2lox targeting vector. The inducible Pax7 ES cell line was generated in A2Lox.cre ES cells, an improved version of A2Lox[29], in which cre is present at the doxycycline-inducible locus before recombination and catalyzes its replacement by the gene of interest. Inducible expression of Pax7 was assessed by western blot using a monoclonal anti-Pax7 antibody (R&D Systems).

Growth and differentiation of ES cells

Mouse ES cells were maintained and differentiated as described[30]. To induce Pax7 expression during EB differentiation, doxycyclin (Sigma) was added to the cultures at 1μg/ml beginning at day 2 of EB differentiation. To assess the presence of myogenic precursors in these cultures, intact EBs were collected and plated in a 10cm dish in the same medium (± dox). Outgrowths were then further evaluated for myogenic differentiation as described[27].

FACS analysis and sorting of EB-derived cells

EB cells were collected after a short incubation with Trypsin or PBS without calcium and magnesium supplemented with 1mM EDTA and 0.5% BSA, washed twice, first with IMDM 10% FBS and then with staining buffer (PBS 2% FBS), suspended in the same buffer containing 0.25μg/10^6 cells of Fc block (Pharmingen). The following antibodies were added at 1μg/10^6 cells in 100 μl of staining buffer, and incubated at 4°C for 30 minutes before washing with the same buffer. For PDGFαR and Flk-1, PE- and APC-conjugated antibodies were used, respectively (eBioscience). We used PE-conjugated anti-CD34 (clone RAM34; eBioscience), anti-Syndecan4 (clone KY/8.2; Pharmingen), and anti-CD44 (eBioscience) antibodies. PE-Cy7-conjugated anti-CD29 (clone KMI6; Pharmingen), APC-conjugated anti-CXCR4 (Pharmingen), and mouse anti-M-cadherin (clone 5; Pharmingen) antibodies. For secondary staining in the case of M-cadherin, we used APC-conjugated goat anti-mouse Ig (Pharmingen) at 1μg/10^6 cells in 100 μl of staining buffer. Stained cells were analyzed and sorted on a FACS Aria (Becton–Dickinson) after addition of propidium iodide (Pharmingen) to exclude dead cells.

Labeling of ES cells

iPax7 and iPax3 ES cells were labeled with a lentiviral vector expressing GFP from the ubiquitin C promoter, as previously described[27, 31] or alternatively with a lentiviral vector expressing fire fly luciferase followed by IRES-GFP from the Ubiquitin C promoter. Briefly, vectors were cotransfected with packaging and coat protein constructs Δ8.91 and pVSVG into 293T cells using the FuGENE 6 transfection reagent (Roche). Virus containing supernatant was collected 48 hours after transfection, filtered, and used for transduction of ES cells.

Real Time PCR analysis

Real time PCR for muscle specific genes was performed using probe sets from Applied Biosystems, as follows: Pax3 (Mm00435491_m1), Pax7 (Mm00834079_m1), Myf5 (Mm00435125_m1), MyoD (Mm00440387_m1), Myogenin (Mm00446194_m), MHC (Mm01332493_g1), and GAPDH (Mm99999915_g1).

Transplantation studies

All animals were handled in strict accordance with good animal practice as defined by the relevant national and/or local animal welfare bodies, and all animal work was approved by the University of Minnesota Institutional Animal Care and Use Committee. Six- to eight-week-old C57 BL/10ScSN-Dmd$^{mdx/j}$ (X-linked muscular dystrophy; Jackson Laboratories) mice were used for the *in vivo* studies. Before intramuscular cell transplantation, mice were injured with cardiotoxin, as previously described[27]. For intra-arterial transplantation, following anesthetization of animals with ketamine/xylazine, the contra-lateral femoral artery (left leg) was canulated retrogradely toward the lumbar aorta and then directly injected with cells as previously described[27]. For immuno-suppression, *mdx* mice received a daily dose of 5mg/kg FK 506 (Tacrolimus; Sigma) intra-peritoneally (IP) from the day before cell injection until the time of euthanasia. For the analyses of luciferase-labeled cells *in vivo*, we used 4–6 wks male non-obese diabetic/severely combined immunodeficient (NOD/SCID) mice from Jackson labs. Briefly, 24 hrs after cardiotoxin damage into both tibilalis anterior muscles, luciferase-labeled myogenic progenitors from each cell line (1×10^6 cells/10μl PBS) were injected into left TA muscles, while the right leg received same volume of PBS as negative control.

Bioluminescence imaging

For capturing bioluminescence, a Xenogen' IVIS-100 system was used. Briefly, 15 minutes after intraperitoneal injection of luciferin in 100μl of PBS (1.5mg/kg, GBT biotechnology), images were acquired for 2 minutes and total flux (*p/s*) was used for subsequent data analysis. Images were recorded for 4 weeks after transplantation. Following a second round of cardiotoxin damage, images were captured for 2 more weeks.

Immunofluorescence staining of cultured cells and tissue sections

Engrafted muscles were frozen in isopentane cooled in liquid nitrogen. Serial 8 to 12μm cryosections were collected. For immunofluorescence staining, cells cultured on slides and tissue cryosections were fixed using cold acetone or 4% PFA, permeabilized with 0.3 % Triton X-100 (Sigma) for 15 min. and blocked with 3% BSA or M.O.M blocking reagent (Vector labs) for 1 hr, and then incubated with primary antibodies including GFP (1:250, Abcam), Pax7 (1:20, Hybridoma bank), Myf5 (1:400, SCBT), Myogenin (1:250, clone F5D, BD Biosciences), MyoD (1:250, clone MoAb 5.8A, BD Biosciences), MHC (1:20) and embryonic MHC (1:20, clone F1.652) (both from Developmental Studies Hybridoma Bank), M-cadherin (1:250, Pharmingen), Ki67 (1:500, Abcam) and dystrophin (1:250, Abcam). Alexa fluor 555 goat-anti-rabbit or mouse, 488 goat-anti-chicken and 647 goat-anti- rabbit (all from Molecular probes) were used as secondary antibodies. All secondary antibodies were diluted for 1:750 and incubated for 45 min. at room temperature. DAPI (1:5000, 4,6-diamidino-2-phenylindole; Fluka) was used to counter-stain nuclei.

Single myofiber isolation and staining

For single myofiber staining, we used a method previously described[22].

Muscle digestion for FACS

After harvesting, muscles were minced into small pieces and digested using 0.2% collagenase type I in IMDM for 1 hour at 37° with frequent triturating by pipette. The digested muscles were then filtered, washed, and stained with specific antibodies as described above.

Sorting of GFP$^+$ cells for *in vitro* studies and secondary transplantation

One month after transplantation of ES-derived myogenic progenitors *mdx* mice (1×10^6 cells/TA, n=10 for each cell line), engrafted TA muscles were processed as described above and sorted for GFP$^+$ cells. For *in vitro* studies, sorted cells were cultured under proliferative myogenic medium containing bFGF and chicken extract in the presence or absence of Dox for a period of 2 weeks, at which point, dox-induced cultures were switched to myogenic differentiation conditions. For secondary transplantations, 5000 GFP$^+$ sorted cells/10μl PBS were injected into left TAs of secondary *mdx* mice, while right TAs received PBS (n=4 mice for each cell line). One month later, mice were analyzed for dystrophin and GFP expression.

Muscle preparation for mechanical studies

For the measurement of contractile properties, mice were anaesthetized with avertin (250 mg/kg I.P.) and intact tibialis anterior (TA) muscles were dissected and placed in an experimental organ bath filled with mammalian Ringer solution containing (mM): NaCl 120.5; NaHCO3 20.4; glucose 10; KCl 4.8; CaCl2 1.6; MgSO4 1.2; NaH2PO4 1.2; pyruvate 1.0, adjusted to pH 7.4. The chamber was perfused continuously with 95% O2– 5% CO2 and maintained at a temperature of 25 °C. The muscles were stimulated by an electric field generated between two platinum electrodes placed longitudinally on either side of the muscle (Square wave pulses 25 V, 0.2 ms in duration, 150 Hz). Muscles were adjusted to the optimum length (*Lo*) for the development of isometric twitch force and a 5 min recovery period was allowed between stimulations. Optimal muscle length (*Lo*) and stimulation voltage (25 V) were determined from micromanipulation of muscle length and a series of twitch contractions that produced maximum isometric twitch force. For measuring fatigue time, muscles were stimulated for 1 minute and the time for force to decline to 30% of *Fo* was measured. In brief, after determination of optimal muscle length (*Lo*) and measurement of maximum isometric tetanic force, total muscle fiber cross-sectional area (CSA) was calculated by dividing muscle mass (milligram) by the product of fiber length (millimeter) and 1.06 mg/mm^3, the density of mammalian skeletal muscle. Specific force (*sF*o) was determined by normalizing maximum isometric tetanic force to CSA.

Statistical analysis

Differences between samples were assessed by using the Student's two-tailed t test for independent samples.

RESULTS

Pax7 Induces Myogenesis in Embryoid Body (EB)-Derived Cells

To examine the effect of Pax7 expression on the myogenic differentiation from ES cells, we generated an inducible Pax7 (iPax7) ES cell line using a system similar to that previously described for Pax3[27]. After cre-mediated integration into a doxycycline inducible locus, regulated expression of Pax7 in iPax7 ES clones was confirmed by western blot and immunostaining (Fig. 1A–B). Activation of the myogenic program was observed when dox was added to the culture medium but not in the absence (Fig. 1B). As observed with Pax3[27], sorting for the PDGFαR$^+$Flk-1$^-$ cell fraction on day 5 EBs resulted in a cell population enriched for skeletal myogenic progenitors (Fig. 1C–D). A difference between Pax3 and Pax7 is that expansion of Pax7-induced PDGFαR$^+$Flk-1$^-$-derived monolayers required addition of bFGF to the culture medium (Fig. 1E), as observed for satellite cell proliferation[32], whereas proliferation of Pax3-induced cells did not[27]. Under these proliferation conditions, a majority of Pax7-induced cells expressed Pax7 (95.5 ± 2.3%), Myf5 (79.1 ± 6.8%) and MyoD (46.7 ± 1.2%). Myosin Heavy Chain (MHC), a marker of terminal muscle differentiation, was also present but to a lesser extent (21.3 ± 2.4%) (Fig.

1F, upper panel). This profile changed when cells were exposed to differentiation conditions, which consisted of low glucose DMEM containing 2% horse serum, and withdrawal of dox and bFGF. Under these conditions, most cells expressed MHC (84.4 ± 5.3%) (Fig. 1F, lower panel), and exhibited a typical and uniform morphology of multinucleated myotubes. The majority of the Pax7-induced ES-derived muscle progenitors expressed the surface markers CD44, CXCR4, M-cadherin, CD29, Syndecan-4, Sca-1, and CD34 (Fig. 1G). These two latter antigens were barely or not detected in Pax3-induced cultures[27].

To assess comparatively the potential of Pax3 and Pax7 on the activation of the myogenic program, we performed gene expression analyses on proliferating monolayers obtained from Pax3- and Pax7-induced EB-derived PDGFαR^{+}Flk-1^{-} cells side-by-side. As expected, both Pax3 and Pax7 efficiently activated the myogenic program as evidenced by the up-regulation of Myf5, MyoD, and Myogenin (Fig. S1). In this system, there is no cross-induction between Pax3 and Pax7, as Pax3 expression is undetectable in Pax7-induced cultures and vice-versa (Fig. S1).

Next we compared the *in vivo* regenerative potential of Pax7-induced ES-derived myogenic progenitors to their Pax3-induced counterparts by transplanting them into cardiotoxin-injured *mdx* mice, a mouse model for Duchenne's muscular dystrophy characterized by the deficiency of dystrophin. In order to track transplanted cells *in vivo*, prior to injection, cells were labeled with GFP by lentiviral transduction. Control tibialis anterior (TA) muscles were injected with PBS (contralateral leg). A group of mice were transplanted with iPax3-derived cells as positive control. Mice were treated with daily IP injection of an immunosuppressive agent (tacrolimus) to prevent rejection of non-isogenic cells. Four weeks following transplantation, TAs were harvested and analyzed for assessment of engraftment. Immunostaining showed the presence of dystrophin^{+} myofibers in muscle sections from mice injected with Pax3- (Fig. 2A, middle panel) or Pax7-induced myogenic progenitors transplanted via intramuscular (Fig. 2A, right panel, and Fig. 2B) or intra-arterial administration routes (Fig. S2). Cryosections from PBS-injected mice presented only sporadic revertant Dystrophin^{+} myofibers (Fig. 2A, left panel). Quantification of Dystrophin^{+} myofibers in *mdx* mice transplanted via intramuscular revealed similar levels of primary engraftment between Pax3- and Pax7-derived cells (15.4% ± 2.09% and 14.1% ± 1.31%, respectively) (Fig. 2C). No tumors were detected within 3 months after cell transplantation (data not shown).

In terms of contractile parameters of treated muscles, Pax7-induced myogenic progenitors demonstrated similar potential to Pax3, as shown by superior isometric tetanic force (Fig. 2D), increased absolute (Fig. 2E), and specific force (Fig. 2F) when compared to their respective contralateral PBS-injected leg. Fatigue time (Fig. 2G–H), weight (Fig. 2I) and CSA (Fig. 2J) were not affected, as previously observed for Pax3 following intramuscular cell transplantation[27].

Satellite Cell Engraftment from Pax3- and Pax7-Induced EB-Derived Cells

To assess to what extent Pax3- and Pax7-induced cells seed the satellite cell compartment and are endowed with the ability to self-renew, we performed *in situ* analyses of single myofibers, characterization of the donor-derived mononuclear fraction by FACS and *ex vivo* expansion, secondary transplantation and response to re-injury (Fig. 3A). As discussed, satellite cells are located beneath the basal lamina closely juxtaposed to the muscle fiber and express Pax7 (Fig. 3B, right panel)[1, 9, 10]. Additional markers to identify these cells, include CD34[6, 7], Syndecan-4[8], and M-cadherin (Fig. 3B, left panel)[33, 34]. Pax3- and Pax7-induced myogenic progenitors that had been labeled with GFP were transplanted into TA muscles of *mdx* mice (total of 4 mice for each cell line). After one month, muscles were harvested,

digested using collagenase, and single myofibers were then analyzed by immunostaining using antibodies to GFP, Pax7, and M-cadherin. As observed in Fig. 3C, distinct levels of chimerism could be observed among single myofibers isolated from transplanted muscles, which varied from no chimerism to high levels of GFP. Co-staining of GFP with Pax7 and M-cadherin revealed the presence of donor-derived satellite cells in single myofibers isolated from *mdx* mice that had been transplanted with either Pax3- (Fig. 3D) or Pax7-induced myogenic progenitors (Fig. 3E). These results were confirmed by staining muscle cryosections of transplanted mice, in which donor-derived $Pax7^+$ cells were also detected at the satellite cell position for both Pax3- and Pax7-engrafted muscles (Fig. 4A).

To address the question whether engrafted satellite cells are in a dormant or activated state, we stained transplanted muscles with Ki67, which identifies cycling cells[35]. Although we could easily detected $Ki67^+$ cells in both control and transplanted muscles (Fig. 4B, red arrows), none of these cells were positive for Pax7 (Fig. 4B, white arrows), suggesting that donor-derived GFP^+Pax7^+, as recipient GFP^-Pax7^+ cells, are in a quiescent state one month after the transplantation. It is important to note that induction was not maintained following cell transplantation, and therefore results reflect the nature of injected cells. In addition to our *in situ* results, a set of transplanted *mdx* mice (2 mice for each cell line) was assessed by FACS analyses. While GFP expression was undetectable in the MNC fraction of control non-transplanted mice (Figs. S3A–B, left), FACS analyses of pooled MNCs isolated from *mdx* mice that had been transplanted in both TAs with Pax3- or Pax7-induced ES-derived myogenic progenitors revealed a very distinctive population of GFP^+ cells (Figs. S3A–B, right). Consistently GFP^+ cells expressed several surface markers that have been associated with satellite cells, including CXCR4[7], M-cadherin[33], CD34[6, 7] , and Sca-1 (Figs. S3A–B, far right panels). Although the latter has being associated with activated satellite cells[36], our results with Ki67 staining do not support the hypothesis that engrafted satellite cells are in an activated state as they are not cycling (Fig. 4B). This discrepancy is probably due to the heterogeneity within the GFP^+ mononuclear fraction, which encompasses not only donor-derived quiescent satellite cells, but also myoblasts and interstitial cells, among others, which are possibly labeled by Sca-1.

To further assess whether ES-derived myogenic progenitors can contribute to the satellite cell compartment, we alternatively used $Pax7^{-/-}$ mice as primary recipients, which are devoid of satellite cells[9, 10]. Although these studies were challenged by the extremely low viability of this strain (most of these mice died between 2 and 4 weeks of age), we succeeded in analyzing several $Pax7^{-/-}$ mice that had been transplanted with Pax3- (n=4) or Pax7- (n=2) myogenic cells at 4 weeks of age. The results from these transplantation experiments confirmed the presence of donor-derived $Pax7^+$ satellite cells in engrafted mice one month after injection (Fig. S4).

In vitro Myogenic Potential of Donor-Derived MNCs

To probe the nature of these GFP^+ cells, we re-isolated donor-derived GFP^+ cells from the muscle mononuclear fraction of *mdx* mice that had been transplanted with Pax3- and Pax7-induced ES-derived myogenic progenitors, and examined their myogenic potential before as well as following their *ex vivo* expansion with and without dox induction for a period of 2 weeks. The myogenic nature of GFP^+ mononuclear cells, from both Pax3- and Pax7-transplanted mice, was confirmed by the ability of freshly sorted engrafted cells to differentiate *in vitro* into MHC^+ multinucleated myotubes (Fig. 5A). When sorted cells were subjected to *in vitro* expansion, outgrowth of a myogenic progenitor population was observed for both Pax3 and Pax7 in the presence and absence of dox (Fig. 5B–D). Although by morphology there were no obvious differences (Fig. 5B), dox-induced *ex vivo* cultured cells were more proliferative than cells cultured in the absence of dox (Fig. 5C), which on the other hand, contained more myotubes. These observations were corroborated by real

time RT-PCR, which revealed that GFP$^+$ MNCs expanded in the absence of dox expressed Myogenin, Dystrophin, and MHC but much lower levels of Pax3, Pax7 and Myf-5 than their Pax3- and Pax7-induced counterparts maintained in the presence of dox (Fig. 5D). When subjected to myogenic differentiation conditions, low glucose DMEM containing 2% horse serum, and withdrawal of dox and bFGF, both Pax3- and Pax7-derived cell preparations expressed high levels of MyoD, Myogenin, Dystrophin, and MHC (Fig. 5D). FACS analysis revealed that dox-treated cells showed greater expression of CXCR4 and M-cadherin (Fig. S5). Taken these data together, we conclude that the GFP$^+$ mononuclear cells are myogenic.

Regenerative Potential of Engrafted GFP$^+$ MNCs

To test for self-renewal *in vivo*, we performed secondary transplantations into CTX-injured *mdx* mice. Therefore, we performed secondary transplantations directly from engrafted GFP$^+$ cells obtained from primary recipient *mdx* mice that had previously received 10^6 ES-derived cells per TA one month earlier. 5,000 GFP$^+$ cells from iPax3 and iPax7 primary recipients were sorted by FACS and transplanted into the TA muscle of secondary mice (4 *mdx* mice each for iPax3 and iPax7). The contralateral leg of each mouse was injected with PBS as control. One month later, the presence of Dystrophin$^+$GFP$^+$ myofibers was assessed in secondary mice for both iPax3- and iPax7 ES-derived primary GFP$^+$ cells (Fig. 6A). Quantification of Dystrophin$^+$ myofibers indicated significant levels of secondary engraftment with both Pax3- and Pax7-derived mononuclear cells (10.9% ± 0.9% and 10.4% ± 1.5%, respectively) (Figs. 6A and 6B). Additionally, donor-derived GFP$^+$Pax7$^+$ cells were detected at the satellite cell position for both Pax3- and Pax7- secondary transplantations (Fig. 6C). These results demonstrate the presence of a donor-derived self-renewing cell within the mononuclear fraction of mice transplanted with ES-derived myogenic progenitors. First, we transplanted the *ex vivo* cultured GFP$^+$ mononuclear cells described above, but these gave very low levels of engraftment (data not shown). Loss of engraftability following *ex vivo* culture of satellite cells has been noted previously[20].

To investigate whether ES-derived engrafted cells have the ability to respond to new rounds of injury, we transplanted Luciferase/GFP-labeled iPax3- and iPax7- ES-derived progenitors into CTX-injured NOD/SCID recipients, which 4 weeks later were subjected to a second round of CTX injury. Luciferase activity tended to increase gradually and reach a plateau during the first month after transplantation of Pax3-induced cells, while signal from the Pax7-induced ES-derived cells tended to plateau earlier and decline (Fig. 7A). Re-injury caused an initial reduction of bioluminescence, but engrafted cells in both arms proliferated as evidenced by the overall higher levels of Luciferase activity two weeks after injury (Fig. 7A), suggesting that ES-derived engrafted cells are able to respond to re-injury. It is important to note that these mice were not irradiated, and thus, transplanted cells were competing with recipient satellite cells during regeneration. We also performed histological staining for embryonic myosin heavy chain (embMHC), a marker of newly regenerated myofibers (Fig. 7B). The presence of GFP$^+$embMHC$^+$ myofibers, reflecting donor-derived newly-formed myofibers, confirmed the ability of engrafted cells to respond to new rounds of injury. We also detected GFP$^-$embMHC$^+$ myofibers, representing host-derived newly formed myofibers, indicating that ES-derived engrafted cells competed with recipient satellite cells to promote the regeneration of re-injured muscles, as mice were not subjected to irradiation. We also observed GFP$^+$embMHC$^-$ myofibers which represent fibers that were present before the re-injury (Fig. 7B).

DISCUSSION

Here we show that myogenic progenitors obtained from differentiating embryonic stem cells not only contribute to significant functional myofiber engraftment, but also seed the quiescent satellite cell compartment, as indicated by the presence of GFP$^+$Pax7$^+$Ki67$^-$cells

at the satellite cell position of engrafted myofibers (Fig. 4B). Importantly, engrafted cells have the ability to respond to new rounds of injury, competing with resident satellite cells for the generation of newly formed regenerating myofibers (Fig. 7B). These results are corroborated by the secondary transplantation studies which clearly confirm the regenerative ability of donor-derived GFP^+ mononuclear cells. We observed somewhat lower levels of engraftment if compared to some publications involving the transplantation of satellite cells into irradiated recipients[20, 21]. It is important to emphasize that all the transplantation experiments described here involved non-irradiated mice, and thus ES-derived progenitors had to compete with recipient's satellite cells to promote muscle regeneration. Interestingly, Boldrin and colleagues[37] have recently compared the transplantation of satellite cells into irradiated versus non-irradiated *mdx* mice, and observed that the irradiated experimental group contained substantially more donor-derived regeneration (51 ± 26 versus 7 ± 3 $dystrophin^+$ myofibers, respectively).

More recently two studies have claimed effective myogenic engraftment from differentiating ES cells without the use of genetic manipulation[38, 39]. One group transplanted $PDGF\alpha R^+$ cells, presumptive paraxial mesoderm, into nude mice[38], while the other group transplanted cells positive for SM/C-2.6, an antigen expressed by a fraction of muscle mononuclear cells, which include satellite cells, into conditioned *mdx* mice[39]. Despite evidence for engraftment, neither study demonstrated that donor-derived cells are capable of substantial regeneration (dystrophin-positive myofibers) or of improving the contractile properties of engrafted muscles. Moreover, the anti-SM/C-2.6 antibody which seems essential for the purification of putative satellite cell progenitors in these later studies[39] is not publically available, and the antigen is unknown, which limits its application.

Pax3 is first expressed in the presomitic mesoderm (psm), and subsequently in the dermomyotome, preferentially at dorsomedial and ventrolateral lips, and limbs. Pax7 becomes detectable at the central region of the dermomyotome, and limbs, 24 hours after Pax3. While Pax7 expression is maintained throughout adult life, Pax3 is mostly down-regulated from day 13 onwards[34, 40, 41]. The Pax3-null mutation is embryonic lethal due to a number of developmental defects including absence of limb muscles[41–43], while mice lacking Pax7 are viable and present no embryonic muscle defect[44], although their muscle satellite cells are extinguished postnatally[9, 10]. These phenotypes point to distinct spatiotemporal roles for Pax3 and Pax7 in muscle development. Our present findings indicate that despite these developmental differences, both Pax3- and Pax7-induced myogenic progenitors have the ability to self-renew *in vivo* as well as to produce functional myofibers in primary and secondary assays. Although the presence of donor-derived $Pax7^+$ satellite cells has been considered the gold standard for assuring the long-term regenerative ability of a given cell preparation, recent studies suggest that Pax7 may not be as essential as previously thought for adult satellite cells[34]. We observed that some but not all donor-derived cells associated with myofibers expressed Pax7. On the other hand, donor-derived M-$cadherin^+$ cells were easily detected at the satellite cell position of these muscle grafts (Fig. 3). The $Pax7^-$ donor-derived cell population may represent satellite cells that have already committed to differentiate, satellite cells that for some reason, perhaps their embryonic character, do not express or need Pax7, or another type of cell. Along this line, recent evidence suggest that the stem cell pool may be comprised in part of $Pax7^-$ interstitial cells[45]. Further work will determine whether the engrafted mononuclear cell population can be fractionated into cells of distinct functional potential; however it is clear that these engrafted mononuclear cells have significant myogenic regenerative potential. They resemble satellite cells in their ability to respond to re-injury and their ability to engraft secondary recipients.

Although much still needs to be dissected in regard to the nature and regulation of ES-derived myogenic progenitors, the data presented here provide evidence for their long-term repopulation potential. The finding that these cells are able to improve muscle function as well as to seed the muscle stem cell compartment in primary and secondary transplanted mice indicates that a Pax3- or Pax7-engineered ES-cell based strategy may be effective for the treatment of muscular dystrophies.

Supplementary Material

Refer to Web version on PubMed Central for supplementary material.

Acknowledgments

This work was generously supported by the Dr. Bob and Jean Smith Foundation. The project described was also supported by Grant Number AR055299 to RCRP from NIAMS and AG034370 to MK from NIA at the National Institutes of Health. The monoclonal antibody to MHC was obtained from the Developmental Studies Hybridoma Bank developed under the auspices of the NICHD and maintained by the University of Iowa. We thank A. Magli for helpful discussions.

REFERENCES

1. Mauro A. Satellite cells of skeletal muscle fibres. J. Byophys. Biochem. Cytol. 1961; 9:493–496.
2. Bischoff R. Regeneration of single skeletal muscle fibers in vitro. Anat Rec. 1975; 182:215–235. [PubMed: 168794]
3. Konigsberg UR, Lipton BH, Konigsberg IR. The regenerative response of single mature muscle fibers isolated in vitro. Dev Biol. 1975; 45:260–275. [PubMed: 1193298]
4. Lipton BH, Schultz E. Developmental fate of skeletal muscle satellite cells. Science. 1979; 205:1292–1294. [PubMed: 472747]
5. Cornelison DD, Wold BJ. Single-cell analysis of regulatory gene expression in quiescent and activated mouse skeletal muscle satellite cells. Dev Biol. 1997; 191:270–283. [PubMed: 9398440]
6. Beauchamp JR, Heslop L, Yu DS, et al. Expression of CD34 and Myf5 defines the majority of quiescent adult skeletal muscle satellite cells. J Cell Biol. 2000; 151:1221–1234. [PubMed: 11121437]
7. Sherwood RI, Christensen JL, Weissman IL, et al. Determinants of skeletal muscle contributions from circulating cells, bone marrow cells, and hematopoietic stem cells. Stem Cells. 2004; 22:1292–1304. [PubMed: 15579647]
8. Cornelison DD, Filla MS, Stanley HM, et al. Syndecan-3 and syndecan-4 specifically mark skeletal muscle satellite cells and are implicated in satellite cell maintenance and muscle regeneration. Dev Biol. 2001; 239:79–94. [PubMed: 11784020]
9. Oustanina S, Hause G, Braun T. Pax7 directs postnal renewal and propagation of myogenic satellite cells but not their specification. EMBO J. 2004; 23:3430–3439. [PubMed: 15282552]
10. Seale P, Sabourin LA, Girgis-Gabardo A, et al. Pax7 is required for the specification of myogenic satellite cellls. Cell. 2000; 102:777–786. [PubMed: 11030621]
11. Zammit PS, Golding JP, Nagata Y, et al. Muscle satellite cells adopt divergent fates: a mechanism for self-renewal? J Cell Biol. 2004; 166:347–357. [PubMed: 15277541]
12. Halevy O, Piestun Y, Allouh MZ, et al. Pattern of Pax7 expression during myogenesis in the posthatch chicken establishes a model for satellite cell differentiation and renewal. Dev Dyn. 2004; 231:489–502. [PubMed: 15390217]
13. Olguin HC, Olwin BB. Pax-7 up-regulation inhibits myogenesis and cell cycle progression in satellite cells: a potential mechanism for self-renewal. Dev Biol. 2004; 275:375–388. [PubMed: 15501225]
14. Heslop L, Morgan JE, Partridge TA. Evidence for a myogenic stem cell that is exhausted in dystrophic muscle. J Cell Sci. 2000; 113(Pt 12):2299–2308. [PubMed: 10825301]

15. Koenig M, Hoffman EP, Bertelson CJ, et al. Complete cloning of the Duchenne muscular dystrophy (DMD) cDNA and preliminary genomic organization of the DMD gene in normal and affected individuals. Cell. 1987; 50:509–517. [PubMed: 3607877]
16. Hoffman EP, Brown RHJ, Kunkel LM. Dystrophin: the protein product of the Duchenne muscular dystrophy locus. Cell. 1987; 51:919–928. [PubMed: 3319190]
17. Goldspink G, Fernandes K, Williams PE, et al. Age-related changes in collagen gene expression in the muscles of mdx dystrophic and normal mice. Neuromuscul Disord. 1994; 4:183–191. [PubMed: 7919967]
18. Turk R, Sterrenburg E, de Meijer EJ, et al. Muscle regeneration in dystrophin-deficient mdx mice studied by gene expression profiling. BMC Genomics. 2005; 6:98–113. [PubMed: 16011810]
19. Collins CA, Olsen I, Zammit PS, et al. Stem cell function, self-renewal, and behavioral heterogeneity of cells from the adult muscle satellite cell niche. Cell. 2005; 122:289–301. [PubMed: 16051152]
20. Montarras D, Morgan J, Collins C, et al. Direct isolation of satellite cells for skeletal muscle regeneration. Science. 2005; 309:2064–2067. [PubMed: 16141372]
21. Sacco A, Doyonnas R, Kraft P, et al. Self-renewal and expansion of single transplanted muscle stem cells. Nature. 2008; 456:502–506. [PubMed: 18806774]
22. Cerletti M, Jurga S, Witczak CA, et al. Highly efficient, functional engraftment of skeletal muscle stem cells in dystrophic muscles. Cell. 2008; 134:37–47. [PubMed: 18614009]
23. Tanaka KK, Hall JK, Troy AA, et al. Syndecan-4-expressing muscle progenitor cells in the SP engraft as satellite cells during muscle regeneration. Cell Stem Cell. 2009; 4:217–225. [PubMed: 19265661]
24. van der Loo JC, Ploemacher RE. Marrow- and spleen-seeding efficiencies of all murine hematopoietic stem cell subsets are decreased by preincubation with hematopoietic growth factors. Blood. 1995; 85:2598–2606. [PubMed: 7537121]
25. Traycoff CM, Cornetta K, Yoder MC, et al. Ex vivo expansion of murine hematopoietic progenitor cells generates classes of expanded cells possessing different levels of bone marrow repopulating potential. Exp Hematol. 1996; 24:299–306. [PubMed: 8641356]
26. Guenechea G, Segovia JC, Albella B, et al. Delayed engraftment of nonobese diabetic/severe combined immunodeficient mice transplanted with ex vivo-expanded human CD34(+) cord blood cells. Blood. 1999; 93:1097–1105. [PubMed: 9920860]
27. Darabi R, Gehlbach K, Bachoo RM, et al. Functional skeletal muscle regeneration from differentiating embryonic stem cells. Nat Med. 2008; 14:134–143. [PubMed: 18204461]
28. Seale P, Ishibashi J, Scime A, et al. Pax7 is necessary and sufficient for the myogenic specification of CD45+:Sca1+ stem cells from injured muscle. PLoS Biol. 2004; 2:0664–0672.
29. Iacovino M, Hernandez C, Xu Z, et al. A conserved role for Hox paralog group 4 in regulation of hematopoietic progenitors. Stem Cells Dev. 2009; 18:783–792. [PubMed: 18808325]
30. Kyba M, Perlingeiro RC, Daley GQ. HoxB4 confers definitive lymphoid-myeloid engraftment potential on embryonic stem cell and yolk sac hematopoietic progenitors. Cell. 2002; 109:29–37. [PubMed: 11955444]
31. Lois C, Hong EJ, Pease S, et al. Germline transmission and tissue-specific expression of transgenes delivered by lentiviral vectors. Science. 2002; 295:868–872. [PubMed: 11786607]
32. Allen RE, Dodson MV, Luiten LS. Regulation of skeletal muscle satellite cell proliferation by bovine pituitary fibroblast growth factor. Exp. Cell Res. 1984; 152:154–160. [PubMed: 6714317]
33. Irintchev A, Zeschnigk M, Starzinski-Powitz A, et al. Expression pattern of M-cadherin in normal, denervated, and regenerating mouse muscles. Dev Dyn. 1994; 199:326–337. [PubMed: 8075434]
34. Lepper C, Conway SJ, Fan CM. Adult satellite cells and embryonic muscle progenitors have distinct genetic requirements. Nature. 2009; 460:627–631. [PubMed: 19554048]
35. Mackey AL, Kjaer M, Charifi N, et al. Assessment of satellite cell number and activity status in human skeletal muscle biopsies. Muscle Nerve. 2009; 40:455–465. [PubMed: 19705426]
36. Bosnakovski D, Xu Z, Li W, et al. Prospective isolation of skeletal muscle stem cells with a Pax7 reporter. Stem Cells. 2008; 26:194–204.

37. Boldrin L, Zammit PS, Muntoni F, et al. Mature adult dystrophic mouse muscle environment does not impede efficient engrafted satellite cell regeneration and self-renewal. Stem Cells. 2009; 27:2478–2487. [PubMed: 19575422]

38. Sakurai H, Okawa Y, Inami Y, et al. Paraxial mesodermal progenitors derived from mouse embryonic stem cells contribute to muscle regeneration via differentiation into muscle satellite cells. Stem Cells. 2008; 26:1865–1873. [PubMed: 18450822]

39. Chang H, Yoshimoto M, Umeda K, et al. Generation of transplantable, functional satellite-like cells from mouse embryonic stem cells. FASEB J. 2009; 23:1907–1919. [PubMed: 19168704]

40. Goulding MD, Chalepakis G, Deutsch U, et al. Pax-3, a novel murine DNA binding protein expressed during early neurogenesis. EMBO J. 1991; 10:1135–1147. [PubMed: 2022185]

41. Goulding M, Lumsden A, Paquette AJ. Regulation of Pax-3 expression in the dermomyotome and its role in muscle development. Development. 1994; 120:957–971. [PubMed: 7600971]

42. Epstein DJ, Vekemans M, Gros P. Splotch (Sp2H), a mutation affecting development of the mouse neural tube, shows a deletion within the paired homeodomain of Pax-3. Cell. 1991; 67:767–774. [PubMed: 1682057]

43. Bober E, Franz T, Arnold HH, et al. Pax-3 is required for the development of limb muscles: a possible role for the migration of dermomyotomal muscle progenitor cells. Development. 1994; 120:603–612. [PubMed: 8162858]

44. Mansouri A, Stoykova A, Torres M, et al. Dysgenesis of cephalic neural crest derivatives in Pax7−/− mutant mice. Development. 1996; 122:831–838. [PubMed: 8631261]

45. Mitchell KJ, Pannerec A, Cadot B, et al. Identification and characterization of a non-satellite cell muscle resident progenitor during postnatal development. Nat Cell Biol. 2010; 12:257–266. [PubMed: 20118923]

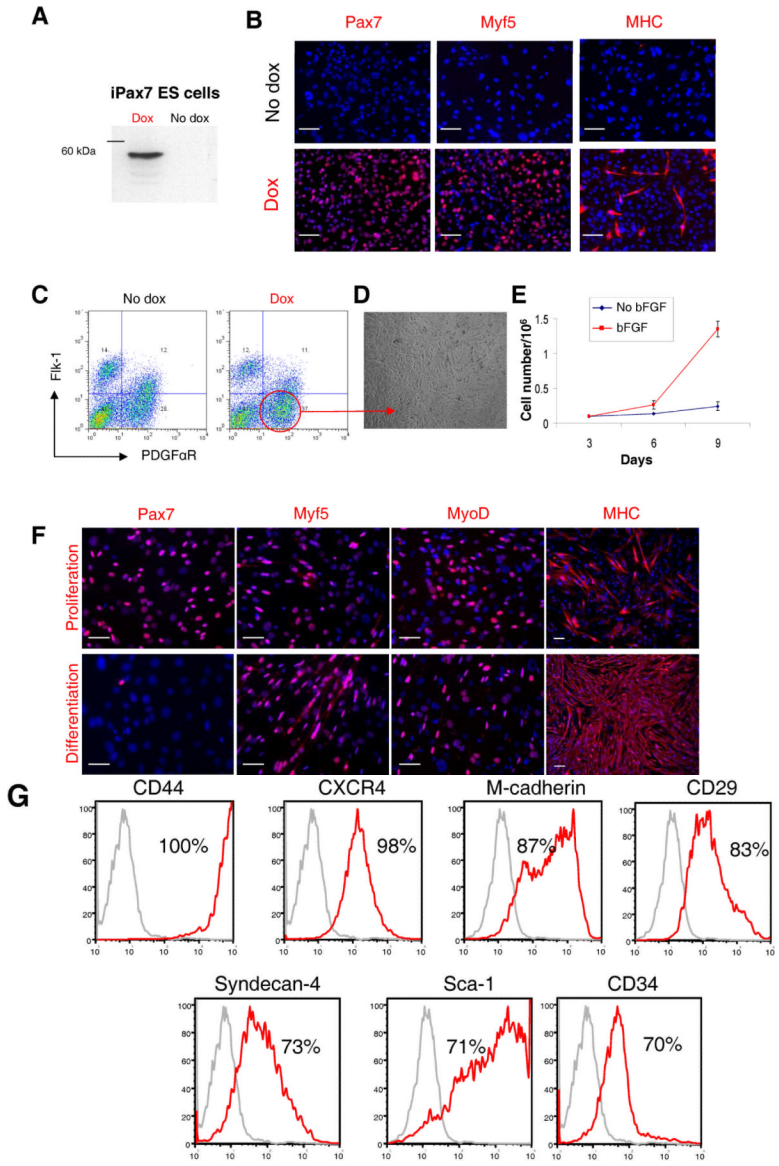

Figure 1. Characterization of *iPax7* ES cells

(A) Western blot for Pax7. **(B)** Immunofluorescence staining of *iPax7* day 5 EB-derived cell monolayers, with (lower panel) and without (upper panel) Pax7 induction. Cells are co-stained with DAPI (blue). Scale bar is 100 μm. **(C)** A representative FACS profile for Flk-1 and PDGFαR expression for *iPax7* ES cells at day 5 of EB differentiation. Dox was added to the EB medium from day 2 to day 5 of EB differentiation (right panel) or not added (left panel). **(D)** Morphology of monolayer resulting from induced *iPax7* cells ten days (p2) after the sorting of the PDGFαR^{+}Flk-1^{-} cell fraction. **(E)** Growth curve of Pax7-induced day 5 EB-derived PDGFαR^{+}Flk-1^{-} cells cultured in EBD medium containing dox ± bFGF. Error bars indicate standard errors from 4 independent experiments. **(F)** Representative images of induced *iPax7* PDGFαR^{+}Flk-1^{-}-derived cells under proliferation (upper panel) and differentiation (lower panel) conditions with staining for Pax7, Myf5, MyoD, and MHC. Cells are co-stained with DAPI (blue). Scale bar is 100 μm. This analysis was performed three times. **(G)** FACS analysis of monolayers obtained from PDGFαR^{+}Flk-1^{-} cells at passage 2. Plots show isotype or secondary control staining profile (gray line) versus

specific antibody staining profile (red line). Percentages represent the fraction of cells that express a given surface antigen. These plots are representative from 4 independent experiments.

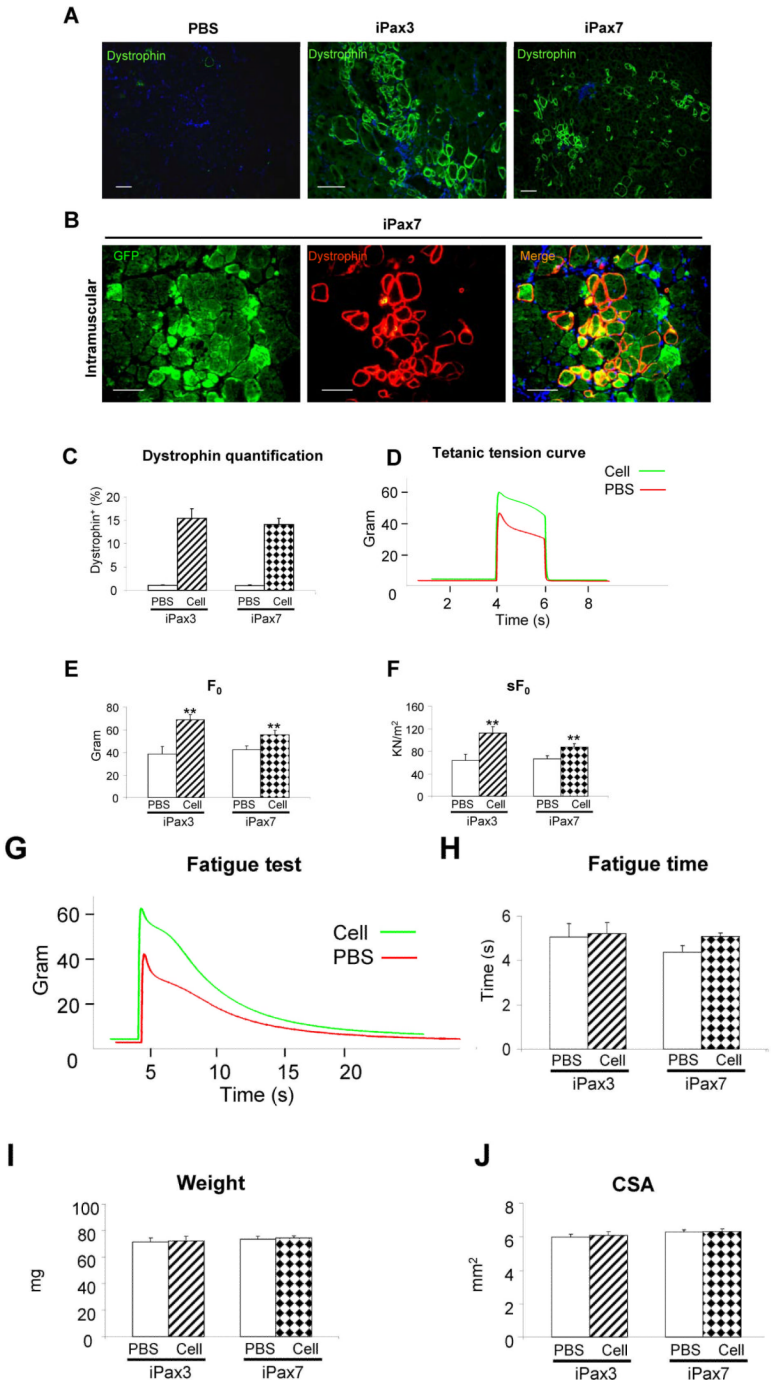

Figure 2. Engraftment ability of Pax7-induced PDGFαR$^+$Flk-1$^-$-derived myogenic progenitors into *mdx* mice

(A) Immunostaining for dystrophin (green) in muscle of CTX-injured mice injected with PBS (contralateral leg; left panel), transplanted with Pax3- (n = 6 mice; middle panel), and Pax7-induced PDGFαR$^+$Flk-1$^-$-derived cells (n = 10; right panel) one month after intramuscular transplantation. Engraftment is demonstrated by dystrophin immunostaining in green. Cells are co-stained with DAPI (blue). Scale bar is 100 μm. **(B)** Higher magnification of a muscle section that had been transplanted with Pax7-induced ES-derived myogenic progenitors shows the presence of GFP$^+$Dystrophin$^+$ myofibers. GFP in green

(left panel), dystrophin in red (middle panel), and merge (right panel). **(C)** Dystrophin quantification of treated mice. For each muscle, five representative cross-sections at 2 mm intervals were counted. For PBS control groups, we examined 20 random sections to enumerate the sporadic revertant Dystrophin^{+} myofibers. **(D)** Representative example of force tracing in TA muscles from *mdx* mice injected with *Pax7*-induced PDGFαR^{+}Flk-1^{-} EB derived cells (green line) or PBS (control, red line). **(E–F)** Effect of iPax3 and iPax7 cell transplantation on absolute and specific (sF_0: F_0 normalized to CSA) force, respectively. **(G)** Representative traces of fatigue test in Pax7- (green) versus PBS-injected muscles (red), in which muscles were stimulated for up to 1 minute, and the time for force to decline to 30% of *Fo* was measured, as shown in **(H). (I–J)** Average weight and CSA of analyzed muscles, respectively. ** $p < 0.01$

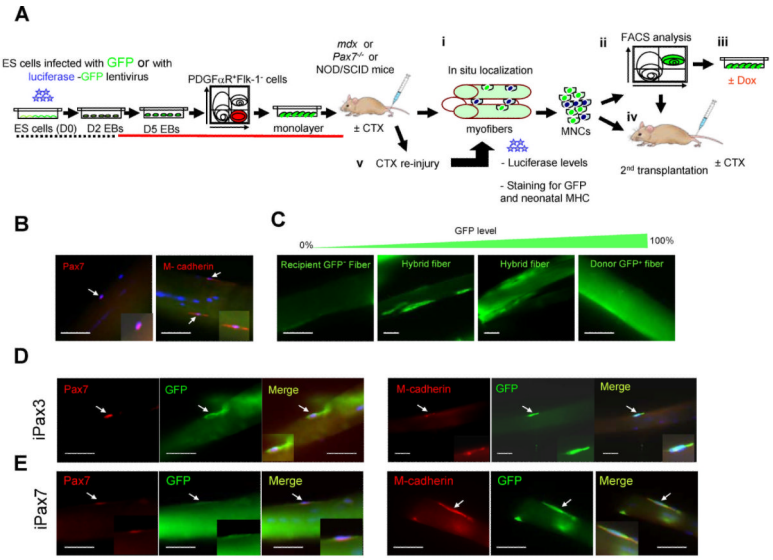

Figure 3. Presence of donor-derived satellite cells following the transplantation of ES-derived myogenic progenitors

(A) Experimental scheme to assess satellite cell-derived engraftment, self-renewal, and regenerative potential of Pax3- and Pax7-induced ES-derived myogenic progenitors. **(B)** *In situ* localization of satellite cells in single myofibers obtained from untreated *mdx* mice (GFP^{-}). Arrows indicate cells expressing the satellite cell markers, Pax7 (left) and M-cadherin (right). **(C)** Representative pictures showing various levels of GFP signal in single myofibers, post-transplant. **(D–E)** Analyses of *mdx* mice four weeks following the transplantation of Pax3- **(D)** or Pax7-induced **(E)** ES-derived myogenic progenitors. Panels show single myofibers stained with GFP (Alexa 488), and Pax7 (Alexa 555) (left panels) or M-cadherin (Alexa 555) (right panels) antibodies, in addition to DAPI **(H–I)**. Scale bar is 100 μm.

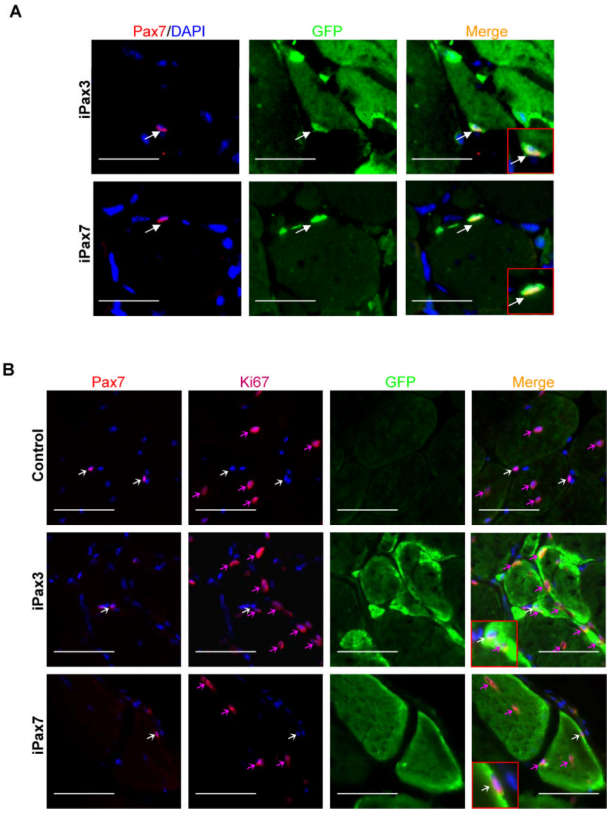

Figure 4. Donor-derived satellite cells are quiescent

(A) *In situ* localization of satellite cells in muscle cryosections obtained from *mdx* mice that had been transplanted with Pax3- (upper panel) or Pax7- (lower panel) induced ES-derived myogenic progenitors, as evidenced by immunostaining for Pax7 in red, GFP in green, and merge for Pax7 and GFP. Arrows indicate $Pax7^{+}GFP^{+}$ cells. **(B)** Co-staining of satellite cells with Ki67 (Alexa 647, far red) to detect cycling cells one month after transplantation. Upper panel shows a representative section of a control TA muscle (GFP^{-}) that had been pre-injured with CTX and injected PBS. White arrows show quiescent satellite cells which express Pax7 (Alexa 555, red) but are negative for Ki67. Note that there are centrally located myofiber nuclei which are proliferating and express Ki67 (red arrows). Middle and lower panels show the presence of donor-derived GFP^{+} myofibers in iPax3 and iPax7-treated muscles, respectively. White arrows indicate donor-derived satellite cells, evidenced by co-expression of Pax7 and GFP, which are negative for Ki67. Red arrows show the presence of cycling $Ki67^{+}$ cells that are negative for Pax7. Scale bar is 100 μm.

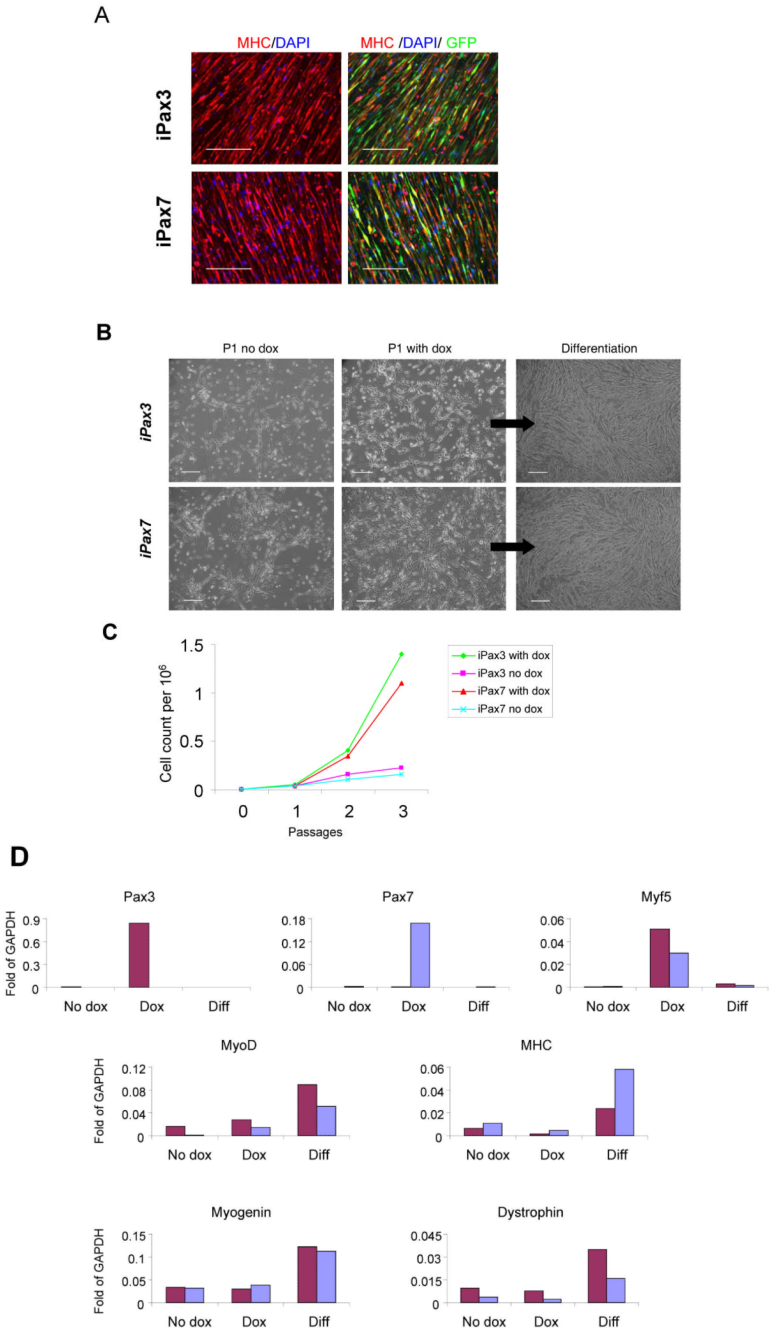

Figure 5. *In vitro* characterization of GFP$^+$ cells sorted from iPax3 and iPax7 transplanted muscles

(A) *In vitro* myogenic differentiation of GFP$^+$ cells isolated from primary transplanted muscles. GFP$^+$ cells sorted out from iPax3- or iPax7-treated muscles (n=4 mice for each cell line), were pulled together and plated onto gelatin-coated plates in the presence of 5ng/ml b-FGF (no dox induction). When cells reached confluency, medium was switched to differentiation conditions (2% HS and bFGF withdrawal). Immunofluorescent staining for MHC (in red) and GFP (green) confirms that GFP$^+$ engrafted mononuclear cells are myogenic, as they have the ability to undergo terminal myogenic differentiation as evidenced by the presence of MHC$^+$GFP$^+$ mature myotubes. Scale bar is 100 μm. **(B)**

Morphology of GFP^+ cells purified from mice that had been transplanted one month earlier with iPax3 (upper panel) and iPax7 (lower panel) ES-derived myogenic progenitors at passage 1 with and without dox, and passage 3 under differentiation conditions (dox withdrawal). Scale bar is 100 μm. **(C)** Representative growth curve of GFP^+ mononuclear cells isolated from iPax3- and iPax7-treated muscles, with and without dox induction, indicates that *ex vivo* Pax3- or Pax7-induction (+ dox) promotes the proliferation of these cells. **(D)** Representative real time PCR of these cells after 2 weeks (3 passages) in culture with and without dox induction and after differentiation (following dox withdrawal). These *in vitro* experiments were performed with pooled GFP^+ mononuclear cells obtained from ten transplanted *mdx* mice for each cell line (both TAs per mouse).

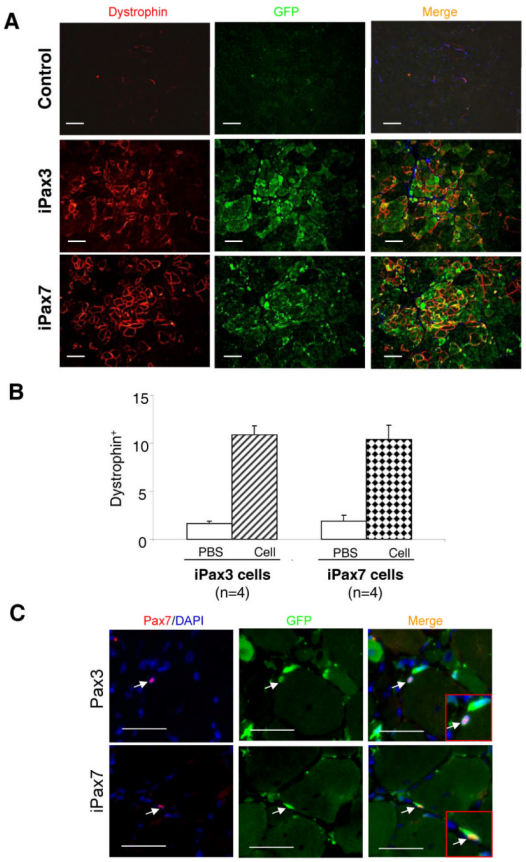

Figure 6. Secondary transplantation of iPax3 and iPax7 ES-derived myogenic progenitors

5000 GFP$^+$ freshly sorted cells from primary *mdx* recipients were injected into the left TA muscle of secondary *mdx* recipients (n=4 for each cell line). Right TAs received the same volume of PBS as control. After 1 month, sections were stained for GFP and Dystrophin. **(A)** The upper row shows a representative section of control TA muscles with few revertant fibers and no GFP signal. Secondary engraftment of GFP$^+$ mononuclear cells isolated from iPax3 (middle panel) and iPax7 (lower panel) transplanted *mdx* mice was demonstrated by immunostaining for dystrophin in red and GFP in green. Cells are co-stained with DAPI (blue). Scale bar is 100 μm. **(B)** Quantification of Dystrophin$^+$ myofibers following primary and secondary transplantation. For quantification, for each muscle, 5 representative cross-sections at 2 mm intervals were counted. For PBS control groups, we examined 20 random sections to enumerate the sporadic revertant Dystrophin$^+$ myofibers. **(C)** *In situ* localization of satellite cells in muscle cryosections obtained from secondary *mdx* mice that had received Pax3- (upper panel) or Pax7- (lower panel) cell preparations, as shown by immunostaining with Pax7 in red, GFP in green, and merge for Pax7 and GFP. Arrows indicate Pax7$^+$GFP$^+$ cells. Scale bar is 100 μm.

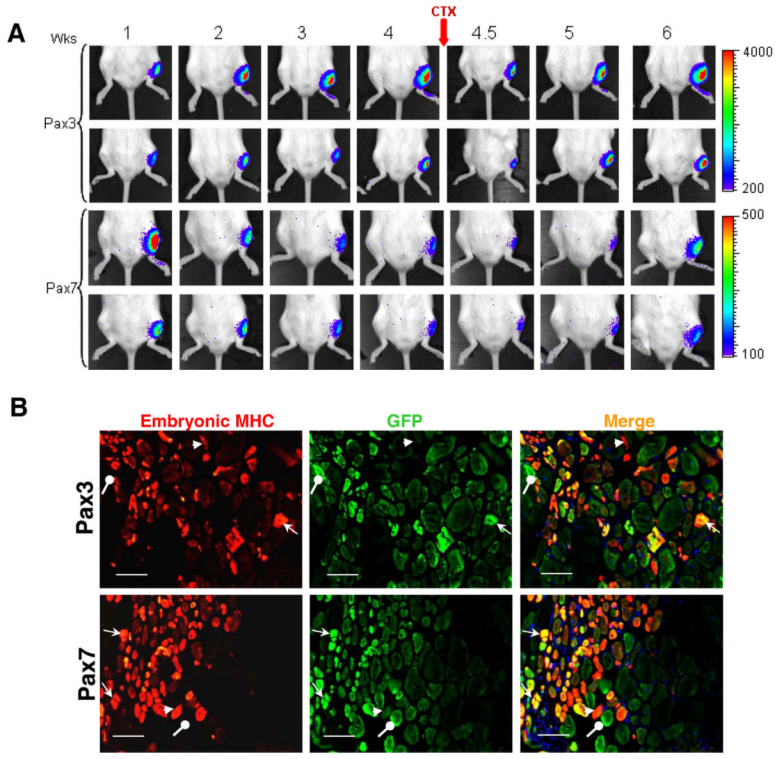

Figure 7. ***In vivo*** **self renewal potential of iPax3 and iPax7 ES-derived myogenic progenitors using the re-injury model**

(A) Bioluminescence images of representative mice from iPax3 and iPax7 groups monitored over 6 weeks. PDGFαR^{+}Flk-1^{-}-derived myogenic progenitors obtained from iPax3 and iPax7 ES cells that had been labeled with a Luciferase-IRES/GFP vector were injected into CTX-injured TA muscles of immunodeficient NOD/SCID mice. After 4 weeks, mice were subjected to CTX re-injury. Scale shows signal intensity. Upper panels show two representative mice for each group. Bioluminescence is shown by total flux (photon per second) during 2 minutes measuring time (n=6 mice per group). **(B)** Immunofluorescence staining of transplanted muscles analyzed 2 weeks after re-injury shows the presence of donor-derived newly formed myofibers as evidenced by co-expression of GFP and embryonic myosin heavy chain. Arrows indicate GFP^{+}embMHC^{+} donor-derived newly-formed myofibers (in yellow/orange), GFP^{-}embMHC^{+} myofibers host derived newly regenerated myofibers (in red), and GFP^{+}embMHC^{-} original donor-derived myofibers (in green). Scale bar is 100 μm.